

REFERENCES AND NOTES

- H. Masuda and K. Fukuda, *Science* **268**, 1466 (1995); R. Gupta, J. J. McClelland, Z. J. Jabbour, R. J. Celotta, *Appl. Phys. Lett.* **67**, 1378 (1995); M. J. Lercollet *et al.*, *J. Vac. Sci. Technol. B* **13**, 1139 (1995); M. Wendel, S. Kuhn, H. Lorenz, J. P. Kotthaus, M. Holland, *Appl. Phys. Lett.* **65**, 1775 (1994); M. A. McCord and D. D. Awschalom, *ibid.* **57**, 2153 (1990); H. Fang, R. Zeller, P. J. Stiles, *ibid.* **55**, 1433 (1989).
- G. M. Whitesides, J. P. Mathias, C. T. Seto, *Science* **254**, 1312 (1991).
- D. Hofstadter, *Phys. Rev. B* **14**, 2239 (1976); D. J. Thouless, M. Kohmoto, M. P. Nightingale, M. den Nijs, *Phys. Rev. Lett.* **49**, 405 (1982).
- D. Weiss *et al.*, *Phys. Rev. Lett.* **66**, 2790 (1991).
- W. Kang, H. L. Stormer, L. N. Pfeiffer, K. W. Baldwin, K. W. West, *ibid.* **71**, 3850 (1993).
- W. D. Volkmuth and R. H. Austin, *Nature* **358**, 600 (1992); W. D. Volkmuth, T. Duke, M. C. Wu, R. H. Austin, A. Szabo, *Phys. Rev. Lett.* **72**, 2117 (1994).
- S. Y. Chou, M. S. Wei, P. R. Krauss, P. B. Fischer, *J. Appl. Phys.* **76**, 6673 (1994).
- T. L. Morkved *et al.*, *Science* **273**, 931 (1996).
- T. L. Morkved, P. Wiltzius, H. M. Jaeger, D. G. Grier, T. A. Witten, *Appl. Phys. Lett.* **64**, 422 (1994).
- P. Mansky, C. K. Harrison, P. M. Chaikin, R. A. Register, N. Yao, *ibid.* **68**, 2586 (1996); P. Mansky, P. Chaikin, E. L. Thomas, *J. Mater. Sci.* **30**, 1987 (1995).
- Z. Li *et al.*, *J. Am. Chem. Soc.* **118**, 10,892 (1996).
- F. S. Bates, *Science* **251**, 898 (1991); ——— and G. H. Fredrickson, *Annu. Rev. Phys. Chem.* **41**, 525 (1990).
- The underlying silicon nitride layer is grown by a plasma-enhanced chemical vapor deposition technique. See S. M. Sze, *VLSI Technology* (McGraw-Hill, New York, ed. 2, 1988), pp. 233–271.
- M. Park *et al.*, in *Symposium Proceedings*, vol. 461, *Morphological Control in Multiphase Polymer Mixtures*, Materials Research Society (MRS), Boston, 2 to 6 December 1996 (MRS, Pittsburgh, PA, 1997), pp. 179–184.
- Because of the discrete microdomain size produced by self-assembly, spin-coated copolymer films on hard substrates rearrange into discrete film thicknesses upon annealing, which typically results in a nonuniform topography [see G. Coulon, D. Ausserre, T. P. Russell, *J. Phys. France* **51**, 777 (1990)]. However, by spin-coating initially at these discrete thicknesses, a uniform film can be produced even after annealing.
- S. M. Sze, *VLSI Technology* (McGraw-Hill, New York, ed. 2, 1988), pp. 184–232.
- The RIE parameters used here are CF₄ (100%), 2 mtorr, 10 standard cubic centimeters per minute (SCCM), 24 W, and ~290 V_{DC} IDC self-bias voltage of cathode (sample holder) with respect to plasma and also CF₄/O₂ (90/10%), 25 mtorr, 20 SCCM, 20 W, and ~170 V_{DC}.
- We obtained the TEM micrographs by spin-coating the copolymer films on thin (~75 nm) silicon nitride windows (50 μm by 50 μm) (Fig. 2). In this way, one can easily image the microdomain morphologies with the substrate intact before RIE and later directly view the patterned silicon nitride after RIE. The high-resolution TEM assists in characterizing and tuning the processing steps. Silicon nitride windows have been previously used in TEM micrography [see (8)]. Having a resolution and contrast of the image but not significantly at the 10-nm length scale.
- The spherical microdomain monolayer shown in Fig. 2A is produced from SB 36/11, which exhibits a cylindrical morphology in bulk. A change from a cylindrical to a spherical morphology in thin films with a few nanometers of variation in film thickness has been observed and discussed previously (14).
- The depth (or height) of the patterned structures is estimated from the etching times and rates (Figs. 2 and 3). In the case of the patterned silicon nitride layer on a silicon substrate in Fig. 3, the estimated number was confirmed by SEM on the cross section of a cracked sample.
- In the case of the osmium-stained copolymer films (Fig. 1C), the addition of O₂ to CF₄ is necessary to obtain an etching selectivity between the PB and PS domains. However, in the case of the ozonated copolymer films (Fig. 1B), a pattern transfer to silicon nitride can be achieved whether pure CF₄ or CF₄/O₂ is used.
- We observed that the discreteness of the microdomain monolayer thickness was less apparent for SI 68/12 when compared with SB 36/11. Even at thicknesses below 70 nm, we observed spherical PI microdomains over the entire sample area but with a poorer order.
- C. Harrison *et al.*, in preparation.
- We have produced a uniform microdomain monolayer template by spin-coating over an entire 76-mm wafer. With a larger ozonator system, the entire wafer would be patterned with the ordered nanostructure arrays.
- We thank P. Mansky for helpful discussions. This project was supported by NSF through the Princeton Center for Complex Materials under grant DMR 9400362. Parts of the processing were carried out at the Advanced Technology Center for Photonics and Optoelectronic Materials at Princeton University and at the Cornell Nanofabrication Center. The silicon nitride windows were fabricated at the Cornell Nanofabrication Center.

3 February 1997; accepted 16 April 1997

Control of Mouse Cardiac Morphogenesis and Myogenesis by Transcription Factor MEF2C

Qing Lin, John Schwarz, Corazon Bucana, Eric N. Olson*

Members of the myocyte enhancer factor–2 (MEF2) family of MADS (MCM1, agamous, deficiens, serum response factor)–box transcription factors bind an A–T–rich DNA sequence associated with muscle-specific genes. The murine *MEF2C* gene is expressed in heart precursor cells before formation of the linear heart tube. In mice homozygous for a null mutation of *MEF2C*, the heart tube did not undergo looping morphogenesis, the future right ventricle did not form, and a subset of cardiac muscle genes was not expressed. The absence of the right ventricular region of the mutant heart correlated with down-regulation of the *dHAND* gene, which encodes a basic helix–loop–helix transcription factor required for cardiac morphogenesis. Thus, *MEF2C* is an essential regulator of cardiac myogenesis and right ventricular development.

The mechanisms that regulate heart formation during embryogenesis are only beginning to be elucidated (1). Members of the MEF2 family of transcription factors bind a conserved A–T–rich DNA sequence associated with most cardiac muscle structural genes (2) and are expressed in cardiogenic precursor cells and differentiated cardiomyocytes during embryogenesis (3). MEF2 factors are also expressed in skeletal and smooth muscle cell lineages (3, 4), and MEF2 binding sites are essential for expression of muscle genes in all three muscle cell types (5).

There are four *MEF2* genes in vertebrate species, designated *MEF2A*, *-B*, *-C*, and *-D*, share homology in an NH₂-terminal MADS-box and an adjacent motif known as the MEF2 domain (5). These protein domains mediate DNA binding, homo- and heterodimerization, and interaction with basic helix–loop–helix (bHLH) transcription factors (6–8).

In the mouse, *MEF2B* and *MEF2C* are

co-expressed in the precardiogenic mesoderm beginning at embryonic day 7.75 (E7.75), and *MEF2A* and *MEF2D* are expressed about 12 hours later (3, 8). *MEF2* gene expression is detected in skeletal muscle precursors in the somites and in smooth muscle cells beginning at about E9.0. Loss-of-function mutations in a single *MEF2* gene in *Drosophila*, *D-mef2*, prevent differentiation of cardiac, skeletal, and visceral muscle cells (9), but the functions of the vertebrate *MEF2* genes in the embryo have not been determined.

To investigate *MEF2C* function during mouse embryogenesis, we inactivated this gene with a targeting vector (10) that deleted the second protein-coding exon, which encodes amino acids 18 to 86 (Fig. 1). The MADS and MEF2 domains are contained in residues 1 to 56 and 57 to 86, respectively, and the residues deleted by the mutation are essential for DNA binding and dimerization (7). The vector was introduced into embryonic stem (ES) cells by electroporation, clones were isolated after positive-negative selection (11), and genomic DNA was analyzed by Southern blot analysis for gene replacement at the *MEF2C* locus (12). The frequency of ES cell clones bearing a targeted *MEF2C* allele was 1:7. Three targeted ES cell clones were injected into blastocysts isolated from C57BL/6J mice to generate chimeras,

Q. Lin and E. N. Olson, Department of Molecular Biology and Oncology, University of Texas Southwestern Medical Center, 5323 Harry Hines Boulevard, Dallas, TX 75235–9148, USA.

J. Schwarz, Division of Cardiology, Department of Internal Medicine, University of Texas Medical School, Houston, TX 77030, USA.

C. Bucana, Department of Cell Biology, University of Texas M. D. Anderson Cancer Center, Houston, TX 77030, USA.

*To whom correspondence should be addressed.

two of which transmitted the mutation through the germ line. Mice heterozygous for the targeted allele showed no discernible phenotype and were intercrossed to obtain *MEF2C* homozygous null offspring. The genotypes of offspring from heterozygous intercrosses were determined within 1 to 3 weeks after birth by Southern blot analysis of DNA obtained from tail biopsies. No neonates homozygous for the *MEF2C* mutation were found among 189 offspring and no neonatal lethality was observed, indicating that the homozygous mutation resulted in embryonic lethality.

We determined the genotypes of embryos between E6.5 and E12.5 by Southern blot or polymerase chain reaction (PCR) analysis (12) of DNA isolated from yolk sacs. Homozygous mutants were detected at roughly the predicted Mendelian frequency between E6.5 and E9.5. Wild-type and mutant embryos were similar in size up to the 14-somite stage (E9.0), and the first branchial arch appeared to form normally in the mutant. However, the mutants developed no more than 20 somites and showed retarded growth after E9.0. No viable mutants were observed by E10.5, indicating that the lethality of the *MEF2C* mutation was fully penetrant by that stage.

The most obvious morphologic defects in mutant embryos were within the heart. The heart develops from bilaterally symmetric cardiogenic primordia that coalesce at the midline to form a primitive heart tube (13). Mutant and wild-type embryos were microscopically indistinguishable at

the linear heart tube stage (E8.0–8.25), and contractions were initiated in the heart tubes of mutants, although they were slower and less rhythmic than normal. At E9.0, the heart rate of wild-type and *MEF2C* heterozygous embryos was 58 ± 3 beats per minute, compared with 26 ± 4 beats per minute for mutants (14). In wild-type embryos, the heart tube initially exhibits a peristaltic beat that becomes sequential after looping, with strong atrial contraction preceding ventricular contraction. In mutants, the atrial chamber exhibited weak contractions, and the hypoplastic ventricular chamber appeared to vibrate only in response to atrial contractions; there was no evidence of independent ventricular contractions. Mutant embryos also exhibited severe pericardial effusion (Fig. 2, A and B), indicative of hemodynamic insufficiency.

At E8.5, the heart tube normally initiates rightward looping, a process that is necessary to orient the atrial and ventricular chambers and to align the outflow tract with the vasculature. Looping morphogenesis is accompanied by formation of the conotruncus in the anteriormost region and later by formation of the common ventricular and atrial chambers. Further maturation of the looped cardiac tube yields the future right and left ventricles and the common atrial chamber. In mutant embryos, the heart tube did not undergo rightward looping (Fig. 2, C to F), and there was no morphologic evidence of the future right ventricle. Rather, a single hypoplastic ventricular chamber was fused directly to an enlarged atrial chamber. Be-

cause of the apparent absence of the future right ventricle, the remaining portion of the ventricular chamber was displaced slightly to the left. The atrioventricular (AV) demarcation was apparent in the mutant, but the AV canal did not elongate. Also, the sinus venosus, which normally forms from the posterior portion of the atrial chamber, did not form in the mutant.

As the ventricular chambers develop, the trabeculae form as fingerlike projections along the inner myocardial wall, which becomes clearly separated from the endocardial layer by a loose mesenchyme called the cardiac jelly. Histological sections of wild-type hearts at E9.0 revealed well-defined atrial and ventricular chambers, with trabeculae projecting from the inner ventricular walls (Fig. 3, A, C, and E). The endocardium was also evident in wild-type embryos at this stage. In mutant hearts, the trabeculae were poorly devel-

Fig. 1. Targeting strategy for the *MEF2C* locus. Diagram of *MEF2C*, which contains 465 amino acids, is shown at the top, above a diagram of the mouse *MEF2C* locus around coding exon 2, which encodes residues 18 to 86. The first intron in the coding region is >10 kb. In the targeting vector (10), the neomycin-resistance gene (*neo*) was transcribed in the same direction as *MEF2C*. Homologous recombination resulted in deletion of coding exon 2. The structure of the targeted allele is shown at the bottom. Insertion of *neo* introduced an Eco RI site that could be used to distinguish the wild-type and mutant alleles. Position of the 3' probe used for Southern blot analysis of yolk sac DNA is indicated. Hybridization of Eco RI-digested DNA with the 3' probe yielded fragments of 11.5 and 3.2 kb from the wild-type and mutant loci, respectively.

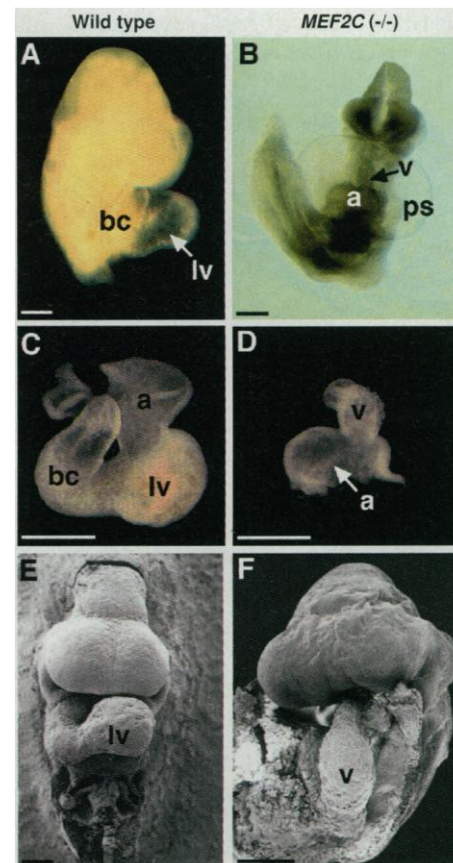
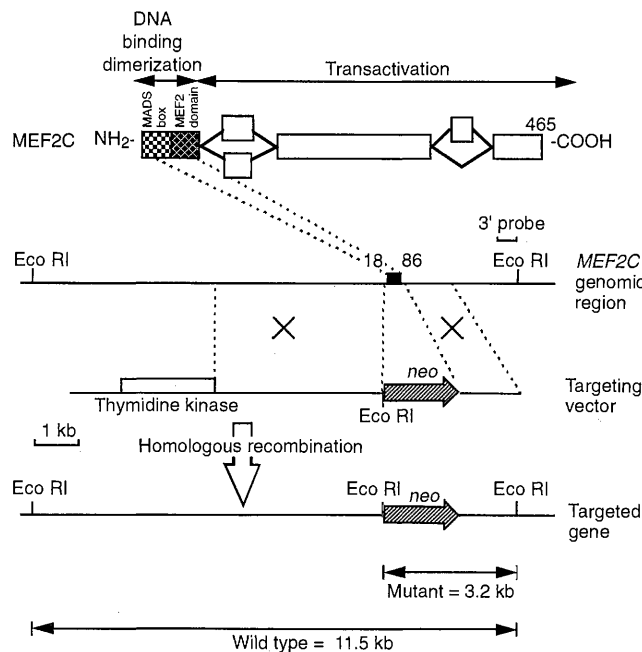


Fig. 2. Cardiac defects in *MEF2C* null embryos. (A) Wild-type and (B) mutant embryos at E9.0. The lower portion of the wild-type embryo was removed for a clear view of the heart. Note severe pericardial effusion in the mutant. Hearts of the wild-type (C) and mutant (D) embryos are shown. Scanning electron micrographs of wild-type (E) and mutant (F) embryos at E9.0. Abbreviations: a, Atrium; bc, bulbus cordis; lv, future left ventricle; ps, pericardial sac; and v, ventricular chamber. Bars = 2 μ m.

oped and the lumen of the ventricular chamber was extremely narrow (Fig. 3, B and F). The cardiomyocytes within the ventricular wall and the endocardial cells also appeared to be disorganized. In the atrial chamber of the mutant, the myocardial wall was thin and the cardiac jelly was absent (Fig. 3D). The AV canal was present in the mutant; however, the endocardial cushions did not form. Red blood cells were seen in the mutant embryos, but very few were present in the heart, suggesting that circulation was impaired. Schematic diagrams showing the morphologies of wild-type and mutant hearts at E9.0 are shown in Fig. 3, G and H, respectively.

Whole mount in situ hybridization of embryos at E9.0, before the mutants began to show retarded growth, demonstrated a reduction in expression of several markers of cardiac differentiation. Transcripts for atrial natriuretic factor (ANF), cardiac α -actin, and α -myosin heavy chain were down-regulated to background levels, and myosin light chain (MLC)-1A expression

was decreased significantly but was still detectable at a low level in the hearts of the mutants (Fig. 4, A to D) (15). In contrast, other cardiac muscle genes, including *MLC2V* (Fig. 4, E and F) and *MLC2A* (15), were expressed at normal levels in the mutants. Expression of *MLC2V* is normally localized to the ventricular region of the developing heart by E9.0 (16). In the mutants, *MLC2V* expression was localized to the hypoplastic ventricular chamber, indicating that the AV chambers were specified correctly.

Quantitative reverse transcriptase-PCR (RT-PCR) (17) confirmed the results of whole mount in situ hybridization and showed that several muscle-specific transcripts were down-regulated four- to fivefold in the mutants. Down-regulation

of the cardiac muscle genes in *MEF2C* mutant embryos was a specific response to the absence of *MEF2C* rather than a secondary result of embryonic demise, because it preceded growth retardation of the embryo and was specific to a certain subset of genes.

The bHLH genes *dHAND* and *eHAND* are expressed in complementary patterns that demarcate distinct regions of the developing mouse heart (18–20). *dHAND* is normally expressed throughout the heart tube before expression becomes localized predominantly to the right side of the looping heart tube (19, 20). In contrast, *eHAND* is expressed in the conotruncus and future left ventricle, but expression is excluded from the region of the heart tube that gives rise to the right ventricle (18–20). In the *MEF2C*

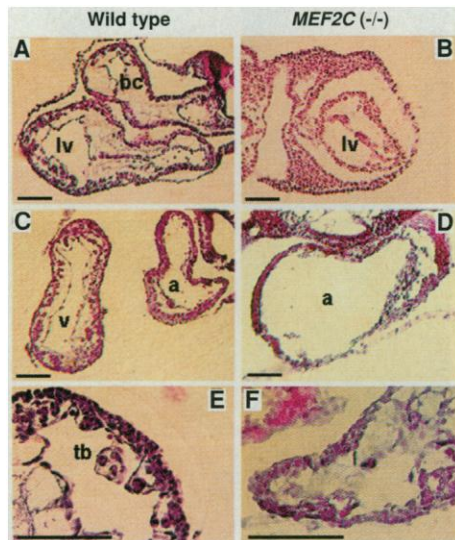


Fig. 3. Hematoxylin and eosin staining of thin sections of hearts of wild-type and mutant embryos. Wild-type (A, C, and E) and mutant (B, D, and F) embryos at E9.0 were fixed, sectioned, and stained with hematoxylin and eosin (27). (G and H) Diagrams of planes of section. Abbreviations: a, Atrium; bc, bulbus cordis; hf, headfold; lv, left ventricle; tb, trabeculae; and v, ventricular chamber. Bars = 1 μ m.

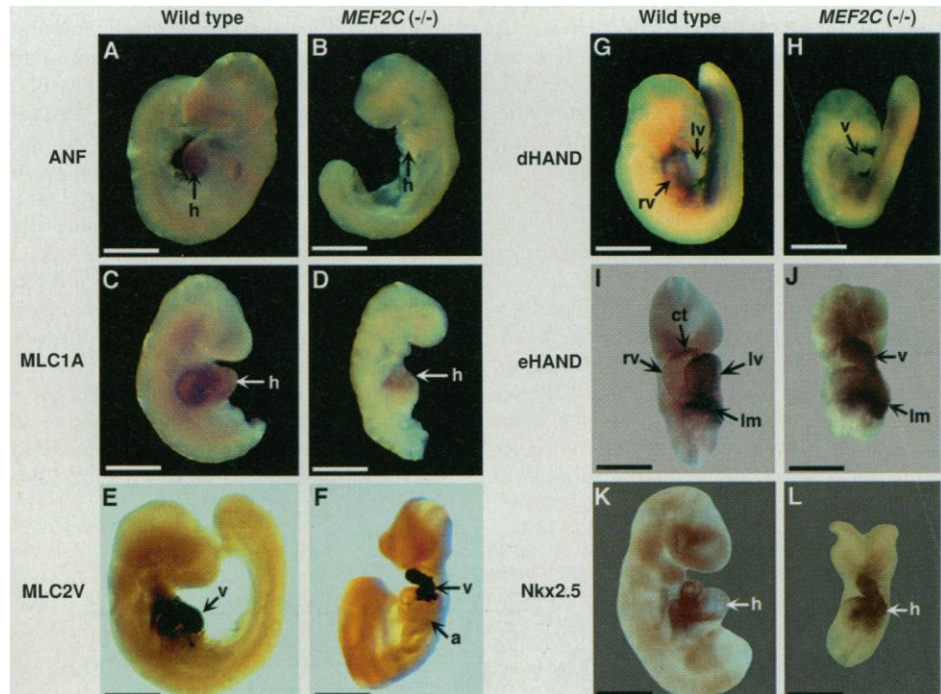


Fig. 4. Analysis of cardiac gene expression by whole mount in situ hybridization. Wild-type (A, C, E, G, I, and K) and mutant (B, D, F, H, J, and L) embryos were stained by in situ hybridization for the indicated transcripts (3, 28). For a clearer view of the heart, heads and tails were dissected away from the embryos in (I), (J), and (L). Note that *dHAND* expression is restricted to the right ventricular region of the heart in the wild-type embryo and is not expressed in the heart of the mutant. *eHAND* is expressed in the conotruncus and left ventricular region in the wild-type heart; in the mutant, there is no gap in expression that would represent the right ventricle. Tails were dissected away from embryos in (C), (D), and (K). (F), (I), (J), and (L) are frontal views; other embryos are viewed from the side. Abbreviations: a, Atrium; ct, conotruncus; h, heart; lv, left ventricle; rv, right ventricle; and v, ventricular chamber. Bars = 5 μ m. (M) Quantitative RT-PCR analysis of gene expression in wild-type (wt) and *MEF2C* mutant (mu) embryos. PCR amplifications were performed with cDNA synthesized from RNA isolated from E9.5 embryonic heart or whole embryos at E8.5 and E9.0 and gene-specific primers for the indicated transcripts. L7 was used as a loading control. Transcripts for *dHAND* were down-regulated in the heart by E9.0, as determined by in situ hybridization. The expression of *dHAND* transcripts in the E8.5 and E9.0 RNA samples used for RT-PCR reflects its expression in the lateral mesoderm and not in the heart. RNA concentrations were quantitated by PhosphorImager analysis.

mutant, *dHAND* was expressed at normal levels in the heart tube before looping (Fig. 4M) (15). However, *dHAND* transcripts were down-regulated at the time of looping, concomitant with failure of the right ventricular region to form (Fig. 4, G, H, and M). *eHAND* was expressed in the mutant, but expression was contiguous throughout the heart tube without the gap in expression that normally characterizes the future right ventricle (Fig. 4, I and J). This distortion in *eHAND* expression and the lack of *dHAND* expression in the heart tube of the mutant are consistent with absence of the future right ventricle. The cardiac homeobox gene *Nkx-2.5* (21) was expressed throughout the developing heart in wild-type and mutant embryos (Fig. 4, K and L). *MEF2B*, which is normally coexpressed with *MEF2C* during the earliest stages of cardiogenesis (3, 8), was up-regulated more than sevenfold in the hearts of mutants at E9.5 (Fig. 4M), whereas *MEF2A* and *MEF2D* transcripts were expressed at comparable levels in wild-type and mutant hearts.

The phenotype of *MEF2C* mutant embryos demonstrates that *MEF2C* is required for looping of the cardiac tube, development of the right ventricle, and expression of a subset of cardiac muscle genes. The cardiogenic defects seen in *MEF2C* mutant embryos are distinct from those seen in other mouse mutants (22) and reveal a cardiogenic regulatory program for right ventricular development.

MEF2C is expressed uniformly throughout the heart tube. Therefore, the selective ablation in the *MEF2C* mutant of the segment of the heart tube that gives rise to the right ventricle suggests that *MEF2C* regulates expression or activity of a regionally restricted regulatory factor required for development of this region of the heart. A candidate for such a factor is the cardiogenic transcription factor *dHAND*, which is expressed throughout the linear heart tube and becomes restricted to the future right ventricle as looping is initiated. Mice homozygous for a null mutation in *dHAND* exhibit a cardiac phenotype similar to that of the *MEF2C* mutant (19), suggesting that *MEF2C* regulates *dHAND* expression in the future right ventricular region of the heart tube or that these two transcription factors cooperate to control right ventricular development, as has been described for *MEF2* and myogenic bHLH proteins in the skeletal muscle lineage (23). *MEF2C* and *dHAND* may control right ventricular development by specifying a subpopulation of cardiogenic cells within the cardiac tube or by regulating the expansion of such a population.

In the absence of *MEF2C*, a subset of

structural genes for cardiac muscle was not up-regulated, whereas others were expressed normally. Some of the cardiac genes that were independent of *MEF2C*, such as *MLC2V*, contain essential *MEF2*-binding sites in their control regions (24), suggesting that downstream genes in the pathway for cardiomyocyte differentiation can discriminate between different members of the *MEF2* family and that another member of the *MEF2* family supports activation of those cardiac genes that are expressed in the *MEF2C* mutant. *MEF2B* is coexpressed with *MEF2C* throughout the early stages of cardiogenesis (3, 8), and it was up-regulated in the *MEF2C* mutant, consistent with the possibility that it may partially substitute for *MEF2C*. That cardiac development occurs normally in *MEF2B*-null mice (25) also suggests that *MEF2C* shares functions with *MEF2B*.

In addition to their expression in the developing heart, members of the *MEF2* family are expressed later in development in skeletal and smooth muscle cells (3, 4, 8), in the nervous system (26), and eventually in a wide range of cell types. *MEF2C* may have additional functions in these other cell types.

REFERENCES AND NOTES

1. E. N. Olson and D. Srivastava, *Science* **272**, 671 (1996); M. C. Fischman and D. Y. R. Stanier, *Circ. Res.* **74**, 757 (1994).
2. L. A. Gossett, D. J. Kelvin, E. A. Sternberg, E. N. Olson, *Mol. Cell. Biol.* **9**, 5022 (1989).
3. D. G. Edmondson, G. E. Lyons, J. F. Martin, E. N. Olson, *Development* **120**, 1251 (1994).
4. A. E. Chambers *et al.*, *Genes Dev.* **8**, 1324 (1994); M. W. Wong, M. Pisegna, M. F. Lu, D. Leibham, M. Perry, *Dev. Biol.* **166**, 683 (1994); B. Nadal-Ginard and S. V. Subramanian, *Mech. Dev.* **57**, 103 (1996); A. B. Firulli *et al.*, *Circ. Res.* **78**, 196 (1996).
5. E. N. Olson, M. Perry, R. A. Schulz, *Dev. Biol.* **172**, 280 (1995).
6. R. Pollock and R. Treisman, *Genes Dev.* **5**, 2327 (1991); J. F. Martin *et al.*, *Mol. Cell. Biol.* **14**, 1647 (1994); J. F. Martin, J. J. Schwarz, E. N. Olson, *Proc. Natl. Acad. Sci. U.S.A.* **90**, 5282 (1993); Y. T. Yu *et al.*, *Genes Dev.* **9**, 1388 (1995); R. E. Breitbart *et al.*, *Development* **118**, 1095 (1993); D. Leifer *et al.*, *Proc. Natl. Acad. Sci. U.S.A.* **90**, 1546 (1993); J. C. McDermott *et al.*, *Mol. Cell. Biol.* **13**, 2564 (1993).
7. J. D. Molkentin *et al.*, *Mol. Cell. Biol.* **16**, 2627 (1996); Y.-T. Yu, *J. Biol. Chem.* **271**, 24675 (1996).
8. J. Molkentin *et al.*, *Mol. Cell. Biol.* **16**, 3814 (1996).
9. B. Lilly *et al.*, *Science* **267**, 688 (1995); B. A. Bour *et al.*, *Genes Dev.* **9**, 730 (1995); G. Ranganayakulu *et al.*, *Dev. Biol.* **171**, 169 (1995).
10. The *MEF2C* targeting vector was constructed as shown in Fig. 1, with the neomycin resistance gene under control of the phosphoglycerol kinase promoter in the same transcriptional orientation as *MEF2C*. A thymidine kinase gene under control of the herpes simplex virus promoter pMC1-HSVtk [S. L. Mansour, K. R. Thomas, M. R. Capecchi, *Nature* **336**, 348 (1988)] was cloned into an Xho I site immediately 5' of the 5' arm of genomic homology. All the cloning junctions in the targeting vector were confirmed by DNA sequencing. The targeting vector was linearized by digestion with Not I before electroporation.
11. The *MEF2C* targeting vector was introduced by electroporation into 129 ES cells [A. P. McMahon and A. Bradley, *Cell* **62**, 1073 (1990)]. After positive-negative selection, surviving clones were isolated and replica-plated onto SN76/7 fibroblasts in 96-well microtiter plates, and genomic DNA was analyzed on Southern blots.
12. Homologous recombination at the *MEF2C* locus was detected by Southern blot or PCR analysis of genomic DNA isolated from ES cells, yolk sacs, or tail biopsies. For Southern blots, genomic DNA was digested with Eco RI and hybridized to a probe from a region immediately 3' of the region of homology used for targeting. For PCR, the following oligonucleotide primers were used: neo primer, 5'-GGCAT-GCTGGGGATGCGGTGGGCTC-3'; *MEF2C* MADS box primer, 5'-AGTACAACAGCCGACGAGAG-CCG-3'; and *MEF2C* short-arm primer, 5'-GTCACCTTAAGACATAAAGCACCCCTCC-3'.
13. R. L. DeHaan, in *Organogenesis*, R. L. DeHaan and H. Ursprung, Eds. (Holt Rinehart Winston, New York, 1964), pp. 377-419.
14. Heart rates were determined in E9.0 embryos obtained from timed matings of *MEF2C* heterozygotes. Pregnant females were killed by cervical dislocation; embryos were removed and placed in phosphate-buffered saline at 37°C. Fourteen wild-type and six mutant embryos were analyzed. The average values were statistically significant, as assessed by a standard *t* test.
15. Q. Lin and E. N. Olson, unpublished data.
16. T. X. O'Brien, K. J. Lee, K. R. Chien, *Proc. Natl. Acad. Sci. U.S.A.* **90**, 5157 (1993).
17. For RT-PCR, total RNA was prepared from isolated hearts at E9.5 and from whole embryos at E8.5 and E9.0, treated with ribonuclease-free deoxyribonuclease I, and resuspended in 20 μ l of water. First strand cDNA synthesis was performed with 10 μ l of RNA with Moloney murine leukemia virus reverse transcriptase (BRL) and random primers. PCR amplification was performed with 0.5 μ l of the cDNA, 0.1 μ Ci of [³²P]deoxycytidine triphosphate (dCTP), and gene-specific primers under conditions of linearity for each individual primer set. Most oligonucleotide primers spanned introns. To confirm that samples were not contaminated with genomic DNA, we also performed duplicate PCRs without RT. All PCR products corresponded to the size predicted for the corresponding transcript. PCR cycles were as follows: 99°C for 2 min then 18 to 25 cycles of 96°C for 30 s, 58°C for 30 s, and 72°C for 45 s. PCR products were separated by 6% polyacrylamide gel electrophoresis and quantitated by analysis on a phosphor-imager (Molecular Dynamics).
18. D. Srivastava, P. Cserjesi, E. N. Olson, *Science* **270**, 1995 (1995); P. Cserjesi, D. Brown, G. E. Lyons, E. N. Olson, *Dev. Biol.* **170**, 664 (1995).
19. D. Srivastava, T. Thomas, Q. Lin, D. Brown, E. N. Olson, *Nature Genetics*, in press.
20. C. Biben and R. P. Harvey, personal communication.
21. T. Lints *et al.*, *Development* **119**, 419 (1993).
22. I. Lyons *et al.*, *Genes Dev.* **9**, 1654 (1995); J. Rossant, *Circ. Res.* **78**, 349 (1996).
23. J. D. Molkentin, B. L. Black, J. F. Martin, E. N. Olson, *Cell* **83**, 1125 (1995); S. Kaushal, J. W. Schneider, B. Nadal-Ginard, V. Mahdavi, *Science* **266**, 1236 (1994).
24. J. D. Molkentin and B. E. Markham, *J. Biol. Chem.* **268**, 19512 (1993); S. Navankasattusas, H. Zhu, A. V. Garcia, S. M. Evans, K. R. Chien, *Mol. Cell. Biol.* **12**, 1469.
25. J. Molkentin, Q. Lin, E. N. Olson, unpublished data.
26. G. E. Lyons, B. K. Micales, J. Schwarz, J. F. Martin, E. N. Olson, *J. Neurosci.* **15**, 5727 (1995).
27. J. F. Martin, A. Bradley, E. N. Olson, *Genes Dev.* **9**, 1237 (1995).
28. Sources of probes were as follows: ANF [R. Zeller *et al.*, *Genes Dev.* **1**, 693 (1987)]; *MLC1A* [P. Barton *et al.*, *J. Biol. Chem.* **263**, 12669 (1988)]; *MLC2V* (16); *eHAND* and *dHAND* (18); and *Nkx-2.5* (21).
29. We thank J. Martin for isolating the *MEF2C* genomic clone, A. Tizenor for assistance with graphics, and D. Srivastava and members of the Olson laboratory for helpful discussions. Supported by grants from NIH, the Muscular Dystrophy Association, the American Heart Association, and the Human Frontiers Sciences Program to E.N.O.

5 December 1996; accepted 2 April 1997